

Running title: Bilateral identity of Arabidopsis root pericycle

Name and address of the Corresponding author:

Nussaume Laurent

Laboratoire de Biologie du Développement des Plantes

SBVME, IBEB, DSV, CEA, CNRS, Univ Aix Marseille

Saint Paul lez Durance

F-13108, France

Phone: +33 4 42 25 31 52

Fax: +33 4 42 25 46 56

Email address: lnussaume@cea.fr

Journal research area:

Development and Hormone action

Diarch symmetry of the vascular bundle in *Arabidopsis* root encompasses the pericycle and is reflected in distich lateral root initiation

Boris Parizot^{1,2}, Laurent Laplaze³, Lilian Ricaud^{1,4}, Elodie Boucheron-Dubuisson⁵, Vincent Bayle¹, Martin Bonke⁶, Ive De Smet², Scott R. Poethig⁷, Yka Helariutta⁶, Jim Haseloff⁴, Dominique Chriqui⁵, Tom Beeckman², Laurent Nussaume¹

¹Laboratoire de Biologie du Développement des Plantes, SBVME, IBEB, DSV, CEA, CNRS, Univ Aix Marseille, Saint Paul lez Durance, F-13108, France.

²Department of Plant Systems Biology, Root Development group, V.I.B., Technologiepark 927, B-9052 Gent, Belgium and Department of Molecular Genetics, Ghent University, B-9052 Gent, Belgium.

³Equipe rhizogène, UMR DIA-PC, Institut de Recherche pour le Développement (IRD), 911 Av. Agropolis, 34394 Montpellier Cedex 5, France.

⁴Department of Plant Sciences, University of Cambridge, Downing Street, Cambridge CB2 3EA, UK.

⁵Université Pierre et Marie Curie, site Ivry-le Raphaël, Laboratoire CEMV-EA3494, IFR 83, case 150, 4 place Jussieu, F-75252 Paris, Cedex 05, France

⁶Institute of Biotechnology, University of Helsinki, Helsinki, Finland

⁷Carolyn Lynch Laboratory, Department of Biology, University of Pennsylvania, Philadelphia, PA 19104, USA

Corresponding author: NUSSAUME Laurent, Laboratoire de Biologie du Développement des Plantes, SBVME, IBEB, DSV, CEA, CNRS, Univ Aix Marseille, Saint Paul lez Durance, F-13108 France, Phone : +33 442253152, Fax : +33 442254656, Email address : lnussaume@cea.fr, Web : <http://www-dsv.cea.fr/instituts/>

Footnotes

Financial source: This work was supported by grants from the CEA, the Marie Curie foundation, the IRD and a Tournesol bilateral grant to L. Laplaze and T. Beeckman (n°11532RD).

ABSTRACT

The outer tissues of dicotyledonous plant roots, i.e. epidermis, cortex and endodermis, are clearly organized in distinct concentric layers in contrast to the diarch to polyarch vascular tissues of the central stele. Up to now the outermost layer of the stele, the pericycle has always been regarded, in accordance with the outer tissue layers, as one uniform concentric layer. However, considering its lateral root forming competence, the pericycle is composed of two different cell types with one subset of cells being associated with the xylem, showing a strong competence to initiate cell division while another group of cells, associated with the phloem, appears to remain quiescent. Here, we established, using detailed microscopy and specific *Arabidopsis thaliana* reporter lines, the existence of two distinct pericycle cell types. The analysis of two enhancer trap reporter lines further suggests that the specification between these two subsets takes place early during development, in relation with the determination of the vascular tissues. A genetic screen resulted in the isolation of mutants perturbed in pericycle differentiation. Detailed phenotypical analyses of two of these mutants combined with observations made in known vascular mutants revealed an intimate correlation between vascular organization, pericycle fate and lateral root initiation potency and illustrated the independence of pericycle differentiation and lateral root initiation from protoxylem differentiation. Taken together our data show that the pericycle is a heterogeneous cell layer with two groups of cells set up in the root meristem by the same genetic pathway controlling the diarch organization of the vasculature.

INTRODUCTION

The *Arabidopsis thaliana* root displays two different levels of tissue organization: a concentric organization formed by the ground layers (endodermis /cortex) and the epidermis, and a bilateral symmetry of the diarch vascular bundle consisting of two poles of xylem elements and two poles of phloem elements (Dolan et al., 1993). The outermost layer of the central cylinder or stele is the pericycle, which is traditionally regarded as one extra concentric layer. Indeed, all pericycle cells share common physical properties and form a unique layer of regularly shaped cells in contact with each other by their tangential cell walls (Dolan et al., 1993). During embryogenesis, the pericycle initiates from the same subset of initial cells as the rest of the stele and can be recognized as a distinct concentric layer already formed at heart stage, even before the endodermal and cortical cell files become specified (Scheres et al., 1994). However, many studies in different species have emphasized the differences between pericycle cells according to their position adjacent to the xylem or the phloem poles in terms of cell division competence (Dubrovsky et al., 2000), cell cycle progression (Beekman et al., 2001), cell size (Casero et al., 1989; Dubrovsky et al., 2000), cell surface arabinogalactan-protein distribution and cell wall thickening (Dolan and Roberts, 1995; Casero et al., 1998; Majewska-Sawka and Nothnagel, 2000), methyl blue staining (Toriyama, 2005), plasmodesmatal connections (Wright and Oparka, 1997; Complainville et al., 2003), physical disposition against endodermis cells (Dolan et al., 1993), microtubules content (Hardham and Gunning, 1979), and marker gene expression (Laplaze et al., 2005; Mahonen et al., 2006).

Lateral root development in dicotyledonous plants occurs post-embryonically from pericycle cells and guarantees the spatial development and plasticity of root systems (Torrey, 1950; Celenza Jr et al., 1995; Malamy, 2005). Auxin is unambiguously the main signal inducing pericycle cells to enter lateral root initiation (Casimiro et al., 2003; De Smet et al., 2007). Interestingly, only the subset of the pericycle cells associated to xylem poles are involved in lateral root initiation thus reinforcing the idea that the pericycle is a heterogeneous cell layer. The mechanisms controlling pericycle cells determination and competence for the lateral root initiation are currently unknown. Here we demonstrate, using cytological approaches, that there are two distinct types of pericycle cells. We describe a new enhancer-trap line marker that visualizes this distinction already as early as in the root meristem. Finally, we used genetic approaches to identify mutants altering quantitatively and/or qualitatively pericycle

organization. Our data substantiate the existence of two types of pericycle cells, set up in the root meristem. Furthermore our data show that the diarch determination of both the pericycle and the vasculature are regulated by a common genetic pathway.

RESULTS

Pericycle is made of two different cell types as revealed by cytological analyses

Only few reports have examined the ultra-structural features of the Arabidopsis root pericycle (Dolan et al., 1993; Wright and Oparka, 1997) and a detailed comparison between pericycle cells at the xylem poles versus the ones at the phloem poles is currently completely lacking. Therefore the cytological aspects of both groups of pericycle cells were analyzed by transmission electron microscopy (TEM) in plants grown under normal conditions as well as under lateral root inhibiting and lateral root inducing conditions. Seedlings were germinated on MS- and 1-*N*-naphthylphthalamic acid (NPA)-medium. At 72 hours after germination, part of the seedlings on NPA was transferred to α -naphthaleneacetic acid (NAA) and incubated for 10 hours. In this way three different samples were obtained: untreated roots, roots prevented from lateral root initiation (NPA) and roots of which the entire pericycle is synchronously induced for lateral root initiation by NAA treatment (Himanen et al., 2002). In all samples, sections for comparative TEM analysis were made through the distal part of the differentiation zone.

In the untreated roots, the protoxylem-pole pericycle cells displayed meristematic features with frequently 3 or more vacuoles and a dense cytoplasm containing numerous electron dense ribosomes (Figure 1A). At the phloem pole, all pericycle cells presented a single and large central vacuole and a parietal cytoplasm with less ribosomes, characteristic for a more differentiated status (Figure 1B). An opposite situation was found for NPA-treated seedlings. Whereas the protoxylem-pole pericycle cells reduced their meristematic appearance by acquiring one large central vacuole and a reduction in the number of ribosomes (Figure 1C), the protophloem-pole pericycle cells showed under these conditions a meristematic appearance with a densely stained cytoplasm, the loss of the central vacuole in most of the cells and an enrichment in endoplasmic reticulum (Figure 1D). In some sections we could even notice the result of a recent periclinal cell division event by the appearance of a thin cell wall subdividing a former pericycle cells into two daughter cells (Figure 1D, arrowheads). These divisions are however rare and never give rise to lateral root formation. After transfer to NAA, the situation was pushed over again with the two types of pericycle cells reacting in

an opposite manner. At the xylem poles, the pericycle cells clearly became meristematic with the development of numerous small vacuoles, nuclei with large nucleoli (Figure 1E), while the phloem pericycle cells reacquired parietal cytoplasm and a central vacuole (Figure 1F). These analyses indicate that both types of pericycle cells react differentially and even in an opposite way to lateral root inhibiting versus lateral root inducing conditions.

Pericycle bilateral heterogeneity already occurs in stele initials

Having demonstrated the clear difference between protoxylem-pole and phloem-pole pericycle cells, we used GAL4 enhancer trap lines (see methods) as markers to study further the organization of the root pericycle. The J0121 line (Laplaze et al., 2005) marks pericycle cells associated with xylem poles (Figure 2, A-H) starting from the elongation zone above the root tip (Figure 2C) and expanding in basipetal direction throughout the root (Figure 2B). J0121 GFP expression precedes protoxylem differentiation (data not shown) and is later closely associated with this tissue (Figure 2E). Usually, three contiguous pericycle cell files are expressing GFP (Figure 2D) which are competent to divide and later form lateral root primordia (Kurup et al., 2005). J0121 GFP expression is down-regulated in nascent and developing lateral root primordia (Figure 2F).

Another population of Arabidopsis GAL4 enhancer trap lines (Col-0 background) was screened to identify novel pericycle markers. This led to the identification of the reporter line Rm1007 which express GFP specifically in pericycle associated with xylem pole (Figure 2, I-N) and mainly in 3 contiguous pericycle files (Figure 2L). Compared to J0121, GFP expression was detected earlier in the root tip starting from the initials immediately above the quiescent center cells (Figure 2, K, L). Furthermore, this expression pattern could be detected in heart stage embryos (Figure 2M). This early expression is comparable to the expression pattern observed in young lateral root primordia before emergence (Figure 2J, arrow). It persists in older parts of the root where GFP remains exclusively expressed in pericycle associated with xylem poles (Figure 2N). Unlike J0121, expression is more intense in young tissues and fades away progressively in older parts (Figure 2I). In conclusion, the expression of the GFP enhancer trap marker in both J0121 and Rm1007 lines labelled a subset of cells in the pericycle, associated with the xylem poles, with Rm1007 labelling the xylem pole pericycle from the first initials.

Lateral root initiation, which takes place in the pericycle cells facing xylem poles is regulated by exogenous and endogenous signals (Malamy, 2005). Different experiments were performed to test whether the pericycle cell specification was modified by stresses, nutrients

and hormones conditions. Neither tested nutrients concentrations (phosphate, nitrate and sucrose), nor stress (wounding, heat shock, and drought) resulted in any obvious change of the GFP expression pattern in the J0121 line (see methods, data not shown). J0121 behaviour was also tested against two major hormones involved in root development. Neither auxin, NPA (Figure 2, G, H) nor cytokinin (Supplementary figure 1, A-D) treatments affected the GFP expression pattern of J0121. Similar results were observed with the Rm1007 line, for NPA and NAA treatments (Figure 2J and Supplementary figure 1, E, F). Therefore, even if these treatments induce (auxin, Celenza Jr et al., 1995) or reduce (NPA & cytokinin, Reed et al., 1998; Lohar et al., 2004) root ability to initiate primordia, they appear to have no effect on the spatial organization of the pericycle cells competent for lateral root initiation. We conclude that Rm1007 and J0121 patterns robustly delimit the subset of pericycle cells competent for lateral root initiation and are not perturbed by auxin or cytokinin treatments. This suggests that the specification of different pericycle cells types is not controlled by any of these signals.

Genetic analysis identifies new mutants altered in pericycle bilateral organization

In order to get insight into the mechanisms that specify the different populations of pericycle cells, we performed a genetic screen on J0121 enhancer trap line. For further analysis, J0121 was preferred instead of Rm1007 since variation in the intensity of the GFP was noticed in Rm1007 probably due to epigenetic regulations. 1500 independent F2 progenies of EMS mutagenized seedlings were screened in order to isolate mutants exhibiting qualitative or quantitative alteration of the GFP expression pattern. This led to the identification of 12 mutants showing different phenotypes related to J0121 expression: discontinuity, ectopic expression in pericycle, ectopic expression outside the pericycle and down regulation of GFP expression. Interestingly, most of these mutants showed an alteration in their lateral root initiation ability (Supplementary figure 2). We have focused on two mutants showing a strong and stable phenotype with altered radial pattern of the GFP expression in the pericycle, *lonesome highway* (*lhw*) (Figure 3, D-F) and *impaired vasculature development* (*ivad*) (Figure 3, G-I) as compared with J0121 marker line control (Figure 3, A-C).

Pericycle determination and lateral root initiation potency are intimately correlated with vascular organization in the *lhw* mutant

Two recessive mutant alleles of the previously reported *lhw* mutant (Ohashi-Ito and Bergmann, 2007) were identified in our screen and were therefore named *lhw-6* and *lhw-7*.

Because the two alleles displayed a highly similar phenotype, we will refer to them as “*lhw*” mutation in this paper. The *lhw* mutants present a reduction in primary root growth and in lateral root initiation density (respectively 37% and 47%; Supplementary figure 2). In contrast to the J0121 line, the *lhw* mutants showed only one strand of pericycle cells expressing GFP (Figure 3F). Furthermore, sections made through the mature part of the root revealed that these lines develop only half of the vascular bundle (one xylem pole and one phloem pole) and fewer pericycle cells compared to the control (Figure 3E and supplementary figure 3). This reduction of the circumferential number of pericycle cells does not prevent lateral root formation (Supplemental figure 2). The loss of the diarch organization starts from the meristematic region and is maintained throughout the whole root in these mutants. The number of cells belonging to the outer layers is not significantly different from those found in wild type plants (Supplementary figure 3) and described previously (Dolan et al., 1993). No structural differences could be observed in the lateral root cap and the columella (data not shown), neither at the level of the four quiescent center cells themselves as compared to wild type (Figure 3D). Confocal microscope analysis revealed the expression to be restricted to one strand of 3 contiguous pericycle cell files associated with the xylem pole along the whole root of the plant (supplementary figure 4, A-C). As in J0121, GFP expression is detected before protoxylem fully differentiates (data not shown). To summarize, *lhw* mutants only develop half of the vascular structures and the loss in diarch organization occurs before the differentiation of the vascular elements. This in turn leads to a single strand of GFP expressing pericycle cells in J0121 marker line background.

In order to study the lateral root forming capacity of the pericycle in *lhw* mutants, plants were germinated on medium supplemented with NPA and then transferred to a medium supplemented with NAA to synchronously stimulate lateral root formation along the whole root of the plant, according to the “Lateral Root Inducible System” (Himanen et al., 2002; Vanneste et al., 2005). Both the J0121 marker line and the mutants were initially checked for proper expression of GFP on NPA supplemented medium and no obvious changes could be noticed (Figure 4 A, C). Four days after germination plants were transferred to NAA, inducing divisions in the pericycle. Roots of wild type plants show the common pattern described in literature with lateral roots emerging on both sides of the root along the two strands of GFP (i.e. pericycle cells associated with xylem poles, Figure 4 B, D). In *lhw*, laterals only emerge from one side of the root following the unique strand of GFP. All the observed lateral roots emerged exclusively from the pericycle associated with xylem poles. This experiment demonstrates that pericycle cells competent for lateral root initiation remain

exclusively adjacent to the xylem pole and express exclusively the J0121 GFP marker. Quantitative losses in vascular bundle and pericycle heterogeneity appear intimately correlated: there is a concomitant loss of diarch and bilateral structures in *lhw* mutants.

Protoxylem differentiation is not required for pericycle differentiation and lateral root initiation

The recessive *ivad* mutant shows ectopic GFP expression in the root: the GFP expression extends in the pericycle additionally to the normal pattern, above the differentiation zone in plants grown 4 to 5 days after germination (Figure 3I). Primary root growth is drastically reduced (Supplementary figure 2) and root gravitropism is altered (data not shown). Further analysis revealed that this mutant was dramatically impaired in vascular and endodermis development (Figure 3, G, H). Fewer cells constitute the vascular bundle. Phloem and protoxylem development are altered; these tissues being partially or even fully absent (Figure 3, G,H). In parts of the root where normal J0121 GFP expression was observed, the vascular bundle appears not to be affected by the mutation (data not shown). The endodermis show also similar alterations (Figure 3G: absent, 3H: partially absent). However, regions with altered GFP patterning in the mutants were found where the endodermis was correctly formed. These aspects of the *ivad* phenotype highlight the intimate link between the correct diarch development of the vascular bundle and the proper bilateral symmetry of the pericycle. Whereas the root phenotype of the *lhw* mutants clearly illustrated the relationship between xylem poles and lateral root initiation, we wondered if impaired protoxylem differentiation of the *ivad* mutant would result in aberrant lateral root initiation. Differential interference contrast (DIC) microscope analysis allows the easy distinction between meta- and protoxylem elements in Arabidopsis roots, the first having reticulate and the latter helical cell wall thickenings. DIC analysis of this mutant revealed that lateral root initiation could still proceed in regions where no protoxylem differentiated (Figure 5, D-F). To confirm this observation, J0121 marker GFP expression and lateral root initiation were investigated in one mutant and one transgenic line, respectively *ahp6* and *Pro_{35S}-VND7:SDRX* in which affected protoxylem differentiation was already described (Kubo et al., 2005; Mahonen et al., 2006). The major defect in these mutants is the discontinuous differentiation of the protoxylem along the primary root. In *ahp6* and *Pro_{35S}-VND7:SDRX*, J0121 GFP maker expression and lateral root initiation can happen in front of xylem poles without any need of differentiated protoxylem (Figure 5, G-I and J-L). Moreover, lateral roots emerge with the same frequency in regions with or without a differentiated protoxylem in *aph6* (data not shown). These results show that

a differentiated protoxylem element within the xylem pole (Figure 5, A-C) is not required for proper pericycle differentiation regarding J0121 GFP expression and lateral root initiation.

Suppression of vascular heterogeneity in the *wol* mutant correlates with a loss of heterogeneity in the pericycle

To determine if the qualitative loss in vasculature heterogeneity has consequences on the ability of pericycle cells to divide and form new lateral roots, we used the *wol* mutant (Scheres et al., 1995). Indeed, this mutant presents a defect in procambial cell specification giving rise to a reduced number of cells. As a consequence the phloem is not determined and only protoxylem tissues differentiate in the vascular bundle (Figure 6E, Scheres et al., 1995; Mahonen et al., 2000).

GFP expression in *wol* J0121 cross spreads over the whole pericycle compared to the control (Figure 6, A, D) suggesting that all pericycle cells differentiate in only one type of tissue in the mutant background. Furthermore, *wol* can be described as a non rooting mutant as it makes almost no lateral roots. The ability of *wol* to produce lateral roots under NAA treatment was tested (Figure 6); no organized primordia were observed above the root tip after 48h (Supplementary figure 5 A-D) and neither after 96h (data not shown) treatments as compared with wild type. Microscope observation of root sections revealed that, in this mutant, all pericycle cells are adjacent to protoxylem elements (Figure 6E), expressing GFP (Figure 6D), and able to divide in a periclinal way upon auxin treatment (Figure 6F) but do not form primordia.

DISCUSSION

In *Arabidopsis*, lateral roots originate deep inside the parent root in one layer of cells that surround the vascular tissues: the pericycle (Dolan et al., 1993). Only pericycle cells in contact with xylem poles have the competence to initiate lateral root development (De Smet et al., 2006). This process of lateral root initiation occurs above the root tip in the differentiated zone of the root. The competence to form lateral root is associated with different cell cycle behaviour. The pericycle cells adjacent to the xylem poles were shown to continue to divide after leaving the root apical meristem whereas the other pericycle cells stop dividing (Dubrovsky et al., 2000; Beeckman et al., 2001). Accordingly, xylem pole associated pericycle cells are shorter than the other pericycle cells in the differentiation zone (Beeckman et al., 2001) and differs by their cytological content.

Moreover, the GAL4 enhancer trap lines J0121 is specifically expressed in xylem pole associated pericycle cells thus suggesting the existence of distinct patterns of gene expression for this subset of cells. However, all these differences between xylem pole and phloem pole pericycle cells appear at a distance from the root tip in a mature region of the root where the differentiation of the first vascular elements is fulfilled. This has led to the notion that the lateral root initiation competence of pericycle cells at the xylem poles might rely to some extent on the correct differentiation of the neighbouring protoxylem cells. In this view, the lateral root initiation capacity of the protoxylem pole pericycle cells would be a relatively late achieved characteristic. The same train of thought can be found in the earlier reported “primed pericycle model” (Barlow, 1984; Skene, 2000) wherein all pericycle cells in the root apical meristem are regarded as equivalent and are supposed to differentiate when they leave the meristem in response to a radial factor emitted by differentiated vascular tissues (Figure 7A). A similar mechanism was demonstrated to control the position of legume nitrogen-fixing nodules in front of xylem poles with ethylene produced in the phloem acting as an inhibitory diffusible factor (Heidstra et al., 1997).

However, in contrast to these hypotheses, our results indicate that the positioning of lateral root primordia is most likely controlled by a different mechanism. We used Rm1007 and J0121 enhancer trap lines and the lateral root organogenesis as markers of pericycle cells identity. We show that xylem pole and phloem pole associated pericycle cells represent two distinct cell populations with different cellular characteristics. In particular, we observed differential responses of these cells to auxin. Indeed, exogenous treatment with NPA and NAA induces opposite responses between the cells of the pericycle (by blocking division at the xylem poles whereas the cells in front of phloem poles de-differentiate and appear even able to divide). This suggests that these two kinds of pericycle cells might have differences in auxin transport system, and/or auxin sensitivity. However, up to now no data are available to support this hypothesis.

We demonstrate using enhancer trap lines that these two types of pericycle cells might become specified as early as or coinciding with the formation of the pericycle initials. Moreover, our genetic analysis indicates that pericycle and vasculature determination in the root meristem are controlled by common mechanisms. This is notably illustrated by a concomitant reduction of the cell number of the vasculature and the pericycle in *lhw* and *wol* mutants whereas the external layers present the same number as the wild type (Supplementary figure 3, Dolan et al., 1993). The idea that xylem-pole and phloem-pole pericycle cells are associated with their respective neighbouring vascular tissue type is supported by molecular

and cellular markers shared between vascular tissues and their associated pericycle cells. For instance, AHP6 (Mahonen et al., 2006) is expressed in protoxylem cells and the adjacent pericycle cells from the initials on. Similarly at the cellular level, AGP distribution is mainly detected along the xylem axis (Majewska-Sawka and Nothnagel, 2000) and symplastic plasmodesmata connections occur mainly between the phloem cells, the adjacent sieve elements and the associated pericycle cells (Wright and Oparka, 1997).

Taken together our data suggest a new model of pericycle organization (Figure 7B) where the bilateral organization of the stele, including the pericycle, is set up in the initials and maintained throughout the root as illustrated by the continuous cell files expressing firstly Rm1007 and later J0121 markers. The stele determination is notably dependent on the activity of the *WOL* and *LHW* genes. Both *wol* and *lhw* mutations induce a concomitant loss of one vascular pole and of the associated pericycle. These observations further suggest that the vascular tissue and its associated pericycle would belong to the same morphogenetic field. Later on, the vascular tissues and the pericycle differentiate as illustrated by vessel formation and lateral root initiation competence respectively. The lateral root initiation defect in *wol* mutant plants can either be a direct consequence of defects in cytokinin signalling or result from the loss of the heterogeneity of the pericycle. Quiescent phloem-pole pericycle cells might be needed to border the area of divisions which is required to get proper organogenesis. We therefore argue for the existence of at least 2 different pericycle cell identities that are closely associated with the adjacent vascular elements. These tissues might therefore be regarded as a full member of the stele rather than being considered as one other concentric layer of the root.

Materials and Methods

Used materials

Arabidopsis thaliana (L.) Heynh. Ecotype Columbia (Col-0) and C24 seeds were obtained from the Nottingham Arabidopsis Stock Center. We analyzed the mutants *wol* (Mahonen et al., 2000), *ahp6* (Mahonen et al., 2006), the dominant repression line *Pro_{35S}-VND7:SDRX* (Kubo et al., 2005) (Col-0 backgrounds), and the marker line J0121 (Laplaze et al., 2005) (C24 background). We used promoter fusion *P_{CYCBI;1}:GUS* (Colon-Carmona et al., 1999). Rm1007 was identified in a new screen for GAL4-GFP enhancer trap lines in Col-0 background; 2000 lines were screened, 380 expressed GFP in the root; 57 at least in the

pericycle and 27 specifically in this tissue layer. Out of these 27 lines, 2 labelled a longitudinal subpopulation of cells in this layer.

Growth conditions and treatments

Seeds were surface sterilized and sown on half strength selective MS medium (Murashige and Skoog medium; Sigma® supplemented with 1% sucrose and 0.8% agar) on vertically oriented square plates (Greiner Labortechnik, Kremmünster, Austria). For treatments with N-1-naphthylphthalamic acid (NPA; Duchefa, Haarlem, The Netherlands) or naphthaleneacetic acid (NAA; Sigma-Aldrich, St Louis, MO), 10 µM was added to the Murashige & Skoog medium (MS, Murashige and Skoog, 1962). For treatments with cytokinin (6-Benzylaminopurine BA, Sigma-Aldrich, St Louis, MO), 0.01 µM, 0.1 µM, 0.5 µM, and 1 µM were added to the MS medium. For treatments with variable concentrations of nutrients we used media containing 0.001 mM and 2.5 mM phosphate according to Misson et al. (2004), 0.01 mM and 1 mM nitrate according to Linkhor et al (2002). For treatments with sucrose, 0, 0.02 and 0.15 M doses were added to the MS medium. Germination was obtained by incubating agar plates, after sowing, for 2 days at 4°C in the dark and then by transferring them to continuous light (110 µmol.m⁻².s⁻¹ cool white fluorescence light) at 20°C with 70% humidity. Heat shock and drought stress have been carried out respectively by exposing plants at 40°C for 2h or by dehydrating them on Whatman® 3MM (Whatman, North America) for two hours at 22°C and then transferring back on medium. After transfer, observations were done according to the following time course: 0, 6, 12, 24 hours.

Mutagenesis

J0121 seeds homozygous for the enhancer trap insertion (M0) were chemically mutagenized with 0.25% EMS (Ethyl-Methyl Sulfonate) for 12 hours and then washed 5 minutes with 0.5 M NaOH. Each of the M1 plantlets was grown independently on soil. The mutant selection was carried out on M2 plantlets grown *in vitro* on half strength selective MS medium and screened for GFP patterning with a fluorescence stereomicroscope MZFLIII (Leica, Wetzlar, Germany). Allelism of the mutants was tested by crossing them together and by phenotyping the progeny.

Root length measurements:

Root length was measured from digital images of the plates using the NIH ImageJ 1.34S software (<http://rsb.info.nih.gov/ij/>). Emerged lateral roots were counted using a Leica MZ16 binocular microscope. Experiments were repeated at least two times independently.

Histochemical, histological and microscopic analysis

For whole-mount microscopic analysis, samples were cleared by mounting in a 90% solution of lactic acid (Acros Organics, Geel, Belgium). All samples were analyzed by DIC microscopy (DMLB; Leica Microsystems). For anatomical analysis using light microscopy transverse sections of roots were performed as described in De Smet et al. (2004) (De Smet et al., 2004). For TEM analysis samples were treated according to Himanen et al. (2004). For fluorescence microscopy, whole seedlings were stained with 10 µg/mL propidium iodide (Sigma-Aldrich) and mounted in water under glass cover slips for green fluorescent protein (GFP) and signal analyzed with a 100M confocal microscope equipped with software package LSM 510 version 3.2 (Zeiss, Jena, Germany). Images were collected with a 488-nm emission filter. For stereomicroscopy, whole seedlings were stained with 10 µg/mL propidium iodide (Sigma-Aldrich) for 3 minutes and observed with a stereo fluorescence microscope MZFLIII (Leica, Wetzlar, Germany)

Supplemental data

Supplementary figure 1. Cytokinin treatments on J0121 and NPA/NAA treatments on Rm1007

Supplementary figure 2. Mutagenesis mutants root measurements

Supplementary figure 3. Cell numbers in Wt compared with *lhw* and *wol* mutants

Supplementary figure 4. Confocal characterization of GFP expression in *lhw* mutant

Supplementary figure 5. *wol* pericycle divisions upon NAA treatment

Acknowledgments

The authors thanks Dr. .M. Kubo for providing the *Pro_{35S}-VND7:SDRX*. Dr S. Svistonoff (Equipe Rhizogènèse, IRD Montpellier), L. Jansen (Root Development Group, VIB Gent) and A.P. Mähönen (Utrecht University) for critical reading of the manuscript.

Literature cited:

- Barlow P** (1984) Positional controls in root development. In PW Barlow and DJ Carr Eds, Positional controls in plant development. Cambridge University Press, Cambridge, United Kingdom: 281-318
- Beeckman T, Burssens S, Inze D** (2001) The peri-cell-cycle in Arabidopsis. *J Exp Bot* **52**: 403-411
- Casero P, Casimiro I, Knox J** (1998) Occurrence of cell surface arabinogalactan-protein and extensin epitopes in relation to pericycle and vascular tissue development in the root apex of four species. *Planta* **204**: 252-259
- Casero PJ, García-Sánchez C, Lloret PG, Navascués J** (1989) Changes in cell length and mitotic index in vascular pattern-related pericycle cell types along the apical meristem and elongation zone of the onion root. *Protoplasma* **153**: 85-90
- Casimiro I, Beeckman T, Graham N, Bhalerao R, Zhang H, Casero P, Sandberg G, Bennett MJ** (2003) Dissecting Arabidopsis lateral root development. *Trends Plant Sci* **8**: 165-171
- Celenza Jr JL, Grisafi PL, Fink GR** (1995) A pathway for lateral root formation in Arabidopsis thaliana. *Genes Dev* **9**: 2131-2142
- Colon-Carmona A, You R, Haimovitch-Gal T, Doerner P** (1999) Technical advance: spatio-temporal analysis of mitotic activity with a labile cyclin-GUS fusion protein. *Plant J* **20**: 503-508
- Complainville A, Brocard L, Roberts I, Dax E, Sever N, Sauer N, Kondorosi A, Wolf S, Oparka K, Crespi M** (2003) Nodule Initiation Involves the Creation of a New Symplasmic Field in Specific Root Cells of Medicago Species. *Plant Cell* **15**: 2778-2791
- De Smet I, Chaerle P, Vanneste S, De Rycke R, Inze D, Beeckman T** (2004) An easy and versatile embedding method for transverse sections. *Journal of Microscopy* **213**: 76-80
- De Smet I, Tetsumura T, De Rybel B, Frey NF, Laplaze L, Casimiro I, Swarup R, Naudts M, Vanneste S, Audenaert D, Inze D, Bennett MJ, Beeckman T** (2007) Auxin-dependent regulation of lateral root positioning in the basal meristem of Arabidopsis. *Development* **134**: 681-690
- De Smet I, Vanneste S, Inze D, Beeckman T** (2006) Lateral root initiation or the birth of a new meristem. *Plant Mol Biol* **60**: 871-887
- Dolan L, Janmaat K, Willemsen V, Linstead P, Poethig S, Roberts K, Scheres B** (1993) Cellular organisation of the Arabidopsis thaliana root. *Development* **119**: 71-84
- Dolan L, Roberts K** (1995) Secondary Thickening in Roots of Arabidopsis thaliana: Anatomy and Cell Surface Changes. *New Phytologist* **131**: 121-128
- Dubrovsky JG, Doerner PW, Colon-Carmona A, Rost TL** (2000) Pericycle cell proliferation and lateral root initiation in Arabidopsis. *Plant Physiol* **124**: 1648-1657
- Hardham AR, Gunning BE** (1979) Interpolation of microtubules into cortical arrays during cell elongation and differentiation in roots of Azolla pinnata. *J Cell Sci* **37**: 411-442
- Heidstra R, Yang WC, Yalcin Y, Peck S, Emons AM, van Kammen A, Bisseling T** (1997) Ethylene provides positional information on cortical cell division but is not involved in Nod factor-induced root hair tip growth in Rhizobium-legume interaction. *Development* **124**: 1781-1787
- Himanen K, Boucheron E, Vanneste S, de Almeida Engler J, Inze D, Beeckman T** (2002) Auxin-mediated cell cycle activation during early lateral root initiation. *Plant Cell* **14**: 2339-2351

- Kubo M, Udagawa M, Nishikubo N, Horiguchi G, Yamaguchi M, Ito J, Mimura T, Fukuda H, Demura T** (2005) Transcription switches for protoxylem and metaxylem vessel formation. *Genes Dev* **19**: 1855-1860
- Kurup S, Runions J, Kohler U, Laplaze L, Hodge S, Haseloff J** (2005) Marking cell lineages in living tissues. *Plant J* **42**: 444-453
- Laplaze L, Parizot B, Baker A, Ricaud L, Martiniere A, Auguy F, Franche C, Nussaume L, Bogusz D, Haseloff J** (2005) GAL4-GFP enhancer trap lines for genetic manipulation of lateral root development in *Arabidopsis thaliana*. *J Exp Bot* **56**: 2433-2442
- Linkohr BI, Williamson LC, Fitter AH, Leyser HM** (2002) Nitrate and phosphate availability and distribution have different effects on root system architecture of *Arabidopsis*. *Plant J* **29**: 751-760
- Lohar DP, Schaff JE, Laskey JG, Kieber JJ, Bilyeu KD, Bird DM** (2004) Cytokinins play opposite roles in lateral root formation, and nematode and rhizobial symbioses. *Plant J* **38**: 203-214
- Mahonen AP, Bishopp A, Higuchi M, Nieminen KM, Kinoshita K, Tormakangas K, Ikeda Y, Oka A, Kakimoto T, Helariutta Y** (2006) Cytokinin signaling and its inhibitor AHP6 regulate cell fate during vascular development. *Science* **311**: 94-98
- Mahonen AP, Bonke M, Kauppinen L, Riikonen M, Benfey PN, Helariutta Y** (2000) A novel two-component hybrid molecule regulates vascular morphogenesis of the *Arabidopsis* root. *Genes Dev* **14**: 2938-2943
- Majewska-Sawka A, Nothnagel EA** (2000) The multiple roles of arabinogalactan proteins in plant development. *Plant Physiol* **122**: 3-10
- Malamy JE** (2005) Intrinsic and environmental response pathways that regulate root system architecture. *Plant, Cell & Environment* **28**: 67-77
- Misson J, Thibaud MC, Bechtold N, Raghothama K, Nussaume L** (2004) Transcriptional regulation and functional properties of *Arabidopsis* Pht1;4, a high affinity transporter contributing greatly to phosphate uptake in phosphate deprived plants. *Plant Mol Biol* **55**: 727-741
- Murashige T, Skoog F** (1962) A revised medium for rapid growth and bioassays with tobacco tissue cultures. *Plant Physiol* **15**: 473-497
- Ohashi-Ito K, Bergmann DC** (2007) Regulation of the *Arabidopsis* root vascular initial population by LONESOME HIGHWAY. *Development*: dev.006296
- Reed RC, Brady SR, Muday GK** (1998) Inhibition of auxin movement from the shoot into the root inhibits lateral root development in *Arabidopsis*. *Plant Physiol* **118**: 1369-1378
- Scheres B, Di Laurenzio L, Willemsen V, Hauser MT, Janmaat K, Weisbeek P, Benfey PN** (1995) Mutations affecting the radial organisation of the *Arabidopsis* root display specific defects throughout the embryonic axis. *Development* **121**: 53-62
- Scheres B, Wolkenfelt H, Willemsen V, Terlouw M, Lawson E, Dean C, Weisbeek P** (1994) Embryonic origin of the *Arabidopsis* primary root and root meristem initials. *Development* **120**: 2475-2487
- Skene KR** (2000) Pattern formation in cluster roots: some developmental and evolutionary considerations. *Annals of Botany* **85**: 901-908
- Toriyama H** (2005) On the remarkable phenomena in the root tip of leguminous plants. *Root Research* **14**: 35-40
- Torrey JG** (1950) The Induction of lateral roots by indoleacetic acid and root decapitation. *American Journal of Botany* **37**: 257-264
- Vanneste S, De Rybel B, Beemster GT, Ljung K, De Smet I, Van Isterdael G, Naudts M, Iida R, Gruijsem W, Tasaka M, Inze D, Fukaki H, Beeckman T** (2005) Cell cycle

progression in the pericycle is not sufficient for SOLITARY ROOT/IAA14-mediated lateral root initiation in *Arabidopsis thaliana*. *Plant Cell* **17**: 3035-3050
Wright KM, Oparka KJ (1997) Metabolic inhibitors induce symplastic movement of solutes from the transport phloem of *Arabidopsis* roots. *J Exp Bot* **48**: 1807-1814

Figure 1. TEM analysis of pericycle cells. TEM analysis of pericycle cells at the protoxylem pole (A, C, E) as compared to pericycle cells at the protophloem pole (B, D, F) after growth on control medium (A, B), on NPA (C, D) and on NPA followed by 10 hours of incubation on NAA (E, F). A newly formed periclinally-oriented cell wall in a pericycle cell at the phloem pole on NPA is indicated by two black arrowheads. Nu: nucleolus, pc: pericycle, pP: protophloem pole, pX: protoxylem pole. Bars: 3,5 μm (A-D) and 3 μm (E, F).

Figure 2. Histological analysis of heterogeneous GFP expression in Rm1007 and J0121 enhancer trap lines. (A-H): J0121 analysis. (A) Binocular imaging of a J0121 plantlet 5 days after germination. Confocal imaging of (B, C) mature part and apex respectively, (D) transversal section of mature part, (E) enlargement of the protoxylem and the associated pericycle, (F) lateral root initiation. Expression of the GFP in the root tip of a 5 DAG J0121 plantlet germinated (G) on a medium supplemented with 10^{-5} M NPA, (H) on a non supplemented medium for 2 days and then transferred to a medium supplemented with 10^{-5} M NAA for 24h. Asterisks mark pericycle cells associated with xylem poles. (I-N): Rm1007 analysis. Binocular imaging of a Rm1007 plantlet (I) root tip 5 days after germination, the arrow indicating the quiescent center, (J) mature zone where lateral root formation is induced by transferring a plantlet germinated on non supplemented medium for 2 days to a medium supplemented with 10^{-5} M NAA for 24h. Confocal longitudinal imaging of Rm1007 (K) in a protoxylem plan, (L) in a plan parallel to the phloem in which can be seen 3 cell files of pericycle expressing GFP, (M) during embryo heart stage formation, (N) in the mature root. The eye symbol gives observation axis indication referring to the pericycle cells expressing GFP. Bars: 50 μm (C, I).

Figure 3. Histological study of stele alterations in *lhw* and *ivad* mutants. Transversal sections of 5 DAG embedded plants: (A-C) C24 plants respectively in the differentiation zone and in mature parts of the root, (D, E) *lhw* plants respectively at the level of the four quiescent center cells and in mature part of the root, (G, H) *ivad* plant in mature part of the root. Longitudinal confocal imaging of (F) *lhw* (one section) and (I) *ivad* mutants (z-series stack superposition). Black lines on sections delimit scheme enlargement. Colours: green

(pericycle), blue and stronger blue (xylem and protoxylem), orange (phloem poles). The eye symbol gives observation axis indication referring to the pericycle cells expressing GFP. Bars: 50 μ m.

Figure 4. Lateral root initiation in *lhw* mutant. J0121 (A, B) and *lhw* (C, D) plants 3 days after germination on medium supplemented with 10⁻⁵ M NPA (A, C) and then transferred 4 days on medium supplemented with 10⁻⁵ M NAA (B, D). Asterisks indicate lateral root emergences. The eye symbol gives observation axis indication referring to the pericycle cells expressing GFP. Bars: 100 μ m.

Figure 5. Lateral root initiation in *ivad*, *ahp6* and *Pro_{35S}-VND7:SDRX* mutants does not require differentiated protoxylem. Lateral root initiation in relation with the presence or the absence of fully developed protoxylem elements has been studied in Col0 J0121 (A, B) and in three lines showing alteration in protoxylem differentiation; *ivad* (E, F), *ahp6* J0121 (G-I) and *Pro_{35S}-VND7:SDRX* J0121 (J-L). In Col0 J0121, metaxylem is surrounded by protoxylem (A, C) and lateral root initiation happens in the pericycle adjacent to the protoxylem. In the three displayed mutants, absence of protoxylem surrounding metaxylem can be noticed (E, G, J) and this absence neither prevent GFP expression in pericycle associated with xylem poles (H, K) nor lateral root initiation (D, F, I, L). Fully differentiated protoxylem presence is indicated with blue arrows, absence is indicated with the red symbol. P: Pericycle, pX: protoxylem, X: metaxylem. Bars: 20 μ m.

Figure 6. Auxin treatment on *wol* mutant. Col0 J0121 (A-C) and *wol* J0121 (D-F) have been cultivated (A, B, D, E) 3DAG on non supplemented medium and then (C, F) transferred 48h on supplemented medium with 10⁻⁵ M NAA. Bar: 50 μ m.

Figure 7. Model for stele determination and differentiation in *Arabidopsis*. The model (A) proposed previously (Barlow, 1984; Skene, 2000) introduced a diarch organization of the vascular bundle that becomes determined at the level of stele initials. The differentiation of the vascular tissues will later induce the bipolar specification of the pericycle and the differentiation into different cell populations, one of which is associated with the xylem pole and is competent for lateral root initiation. Here, we propose an alternative model (B) in which the diarch organization affecting both the vascular bundle and the pericycle is determined from the stele initials onwards. The capacity of pericycle cells to give rise to

lateral root primordia occurs later and remains associated with vascular tissues differentiation. Blue and orange colours respectively represent xylem and phloem tissues. Green colour represents the pericycle, with cells associated with the xylem (light green) or the phloem (darker green) tissues.

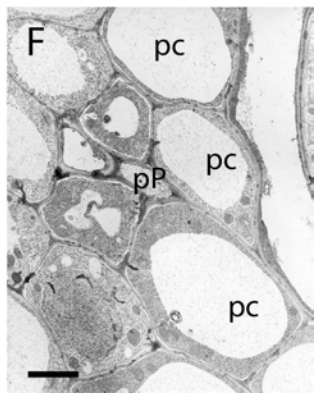
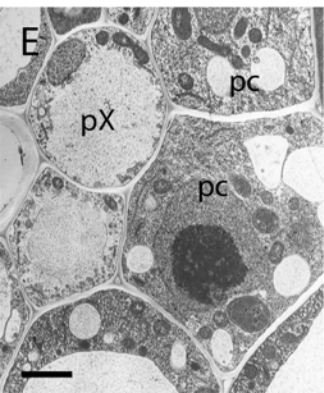
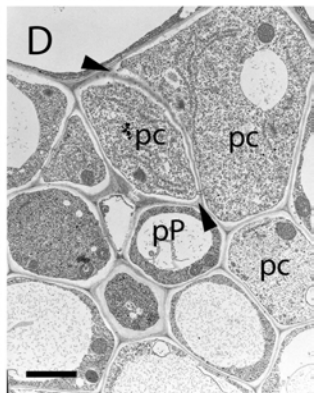
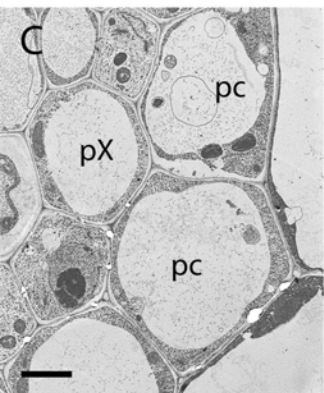
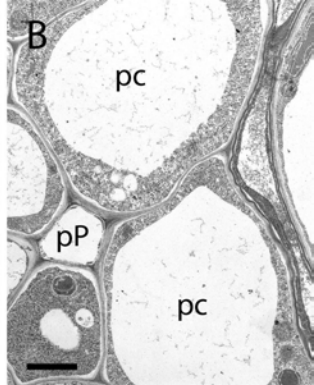
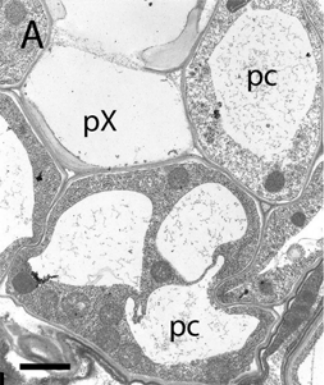
Supplementary figure 1: Cytokinin treatments on J0121 and NPA/NAA treatments on Rm1007. Expression of GFP in the root tip of 5 DAG J0121 plantlets germinated on media respectively supplemented with (A) 0.01, (B) 0.1, (C) 0.5 and (D) 1 μ M BAP. GFP expression in the root tip of 3 DAG Rm1007 plantlets germinated (E) on medium supplemented with 10^{-5} M NPA, (F) on non treated medium for 2 days and then transferred 24h to medium supplemented with 10^{-5} M NAA. Arrows indicate presence of GFP strands i.e. GFP expression in xylem pole associated pericycle. Bar: 100 μ m.

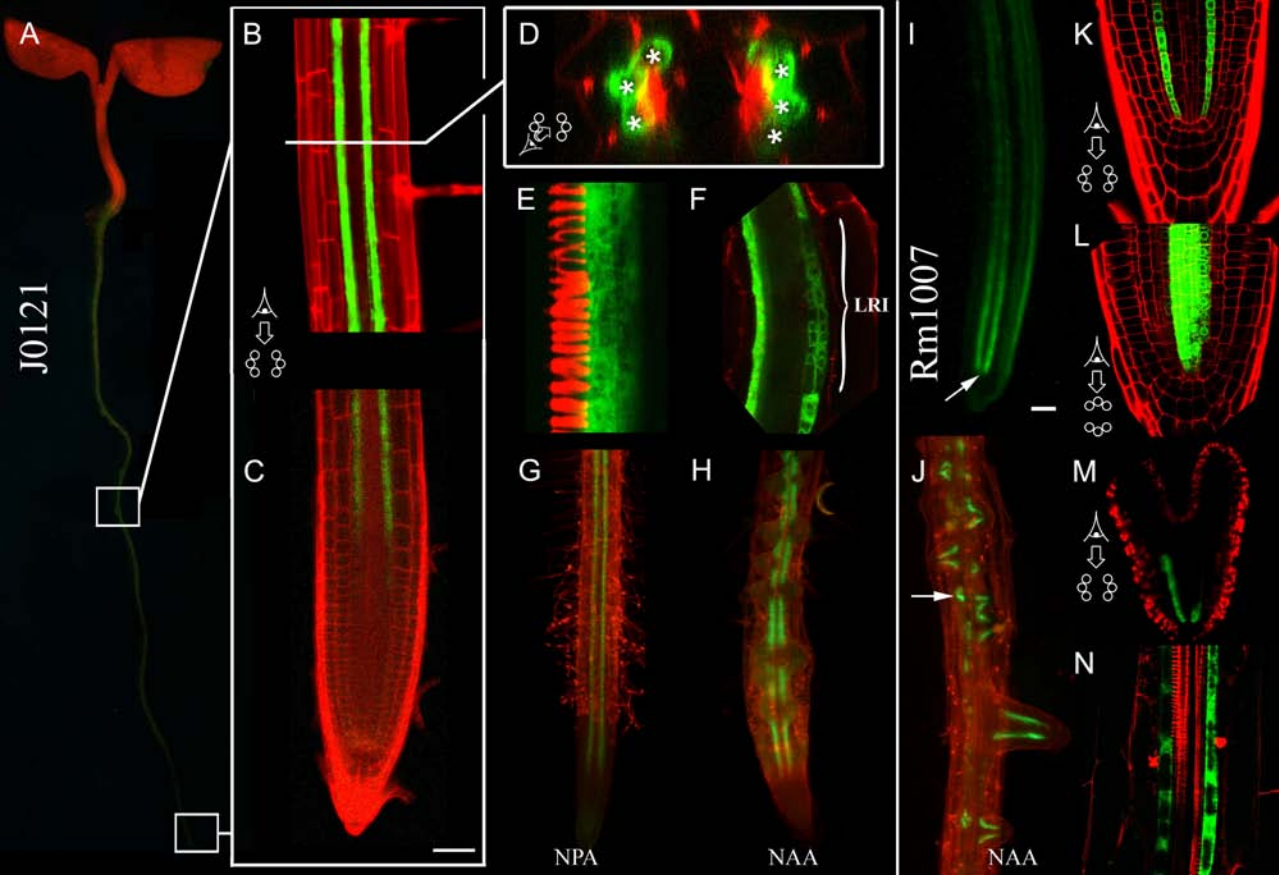
Supplemental figure 2: Mutagenesis mutants root measurements. Primary root length, lateral root number and lateral root density of mutagenesis mutants as compared with the parent control line J0121. All plants (20 plantlets per line) have been grown synchronously under the same condition as the control and measured 12 DAG. Primary root length is indicated in cm and lateral root density is calculated by the ratio between the number of laterals and the primary root length. Asterisks indicate significant difference with the control (student test, $p < 0.01$).

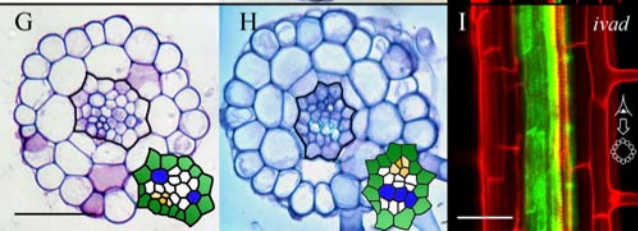
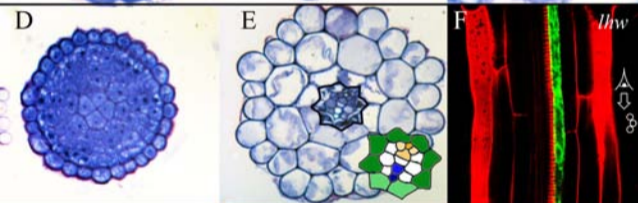
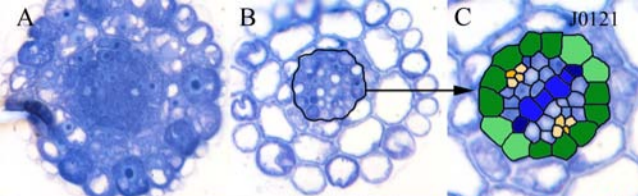
Supplementary figure 3: Cell numbers in Wt compared with *lhw* and *wol* mutants. Cell numbers have been counted on 6 independent plant sections per line, above the root tip, where xylem and phloem fully differentiated. Error bars indicate standard deviation. Scale: cell number, VB: vascular bundle, P: pericycle, E: endodermis, C: cortex, Ep: epidermis. Asterisks indicate significant difference with the control (student test, $p < 0.01$).

Supplementary figure 4: Confocal characterization of GFP expression in *lhw* mutant. Longitudinal imaging: (A) GFP is expressed along the whole root in (B) 3 contiguous pericycle cell files adjacent to xylem poles. Transversal imaging: (C) the GFP is exclusively expressed in front of the xylem poles. The eye symbol gives observation axis indication referring to the pericycle cells expressing GFP. Bar: 50 μ m.

Supplementary figure 5: *wol* pericycle divisions upon NAA treatment. DIC imaging of Wt (A, B) and *wol* (C, D) plantlets cultivated 3 days after germination on MS/2 and then transferred 48h on NAA. Bars: 100µm.







A

J0121

C

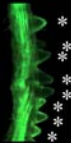
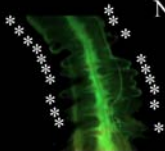
lhw

NPA

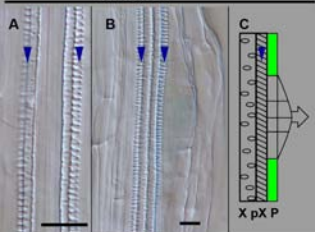
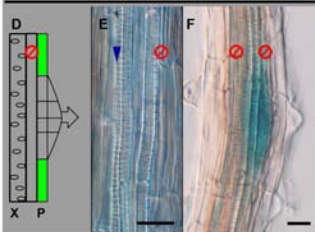
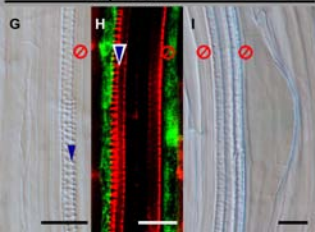
NAA

B

D



Colo J0121

*ivad* CYCB1:GUS*ahp6* J0121*Pro35S-VND7:SDRX* J0121